Laser photolysis study of photochemical reactions of triplet states of pyridinethiones

Maksudul M. Alam, Mamoru Fujitsuka, Akira Watanabe and Osamu Ito *

Institute for Chemical Reaction Science, Tohoku University, Katahira, Aoba-ku, Sendai, 980-77, Japan

Photochemical reactions of pyridine-4(1*H*)-thione (4PyT) and pyridine-2(1*H*)-thione (2PyT) have been studied by nanosecond laser photolysis and steady photolysis methods. The transient absorption bands at 430 and 460 nm are assigned to ^{3}(4PyT)* and ^{3}(2PyT)*, respectively. The lowest triplet energies, triplet lifetimes and quantum yields of intersystem crossing have been determined. Photoinduced electron-transfer reaction from tetramethylbenzidine (TMB) to ^{3}(4PyT)* occurs with a similar rate to that of ^{3}(2PyT)* in a polar solvent. For dinitrobenzene (DNB), an electron-transfer reaction occurred from ^{3}(4PyT)* or ^{3}(2PyT)* to DNB with a diffusion controlled limit. The reactivity of ^{3}(4PyT)* with H-atom donors is higher than that of ^{3}(2PyT)*. The negative ρ-values of the Hammett plots of hydrogen-abstraction rate constants (k_h) from *p*-XC_6H_4SH indicate that ^{3}(2PyT)* is more electrophilic than ^{3}(4PyT)*. From the addition reaction of ^{3}(2PyT)* to various alkenes, the more electrophilic character of ^{3}(2PyT)* than ^{3}(4PyT)* is also confirmed. By comparison of these experimental results with MO calculations, the lowest electronic configurations of ^{3}(4PyT)* and ^{3}(2PyT)* are attributed to ^{3}(n,π*) and ^{3}(π,π*), respectively.

Introduction

The photochemistry of aliphatic thiones and aromatic thiones has been well studied, because of their interesting spectroscopic and photochemical properties.[1–8] Compounds possessing the pyridinethione (PyT) moiety have been widely used for synthetic purposes such as in Barton's reagents.[9–13] They are also biologically active compounds, showing antifungal, antibacterial and anticancer properties.[14–17] The reactivity of a compound to form photogenerated intermediates is frequently pertinent to its biological activity.[18] Photochemical methods are effective for the production of reactive intermediates such as triplet states and radicals with relevance to these reactions and activities. Thus, it is important to investigate the photochemical reactivity of PyT. By employing laser flash photolysis, the electronic structures and reactivities of the photochemical reaction intermediates such as triplet states and radicals can be revealed.[5,19]

The photochemical properties generally originated from the lowest triplet (T_1) and the second excited singlet (S_2) states of thiones.[5,7,8] To investigate the structural influence on the reactivity of the lowest triplet state (T_1) of PyT, we have studied the nanosecond laser-photolysis of pyridine-4(1*H*)-thione (4PyT) and pyridine-2(1*H*)-thione (2PyT) (Scheme 1). Although PyT

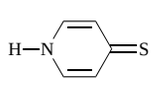

Pyridine-4(1*H*)-thione (4PyT)

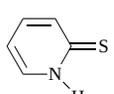

Pyridine-2(1*H*)-thione (2PyT)

are reported to be present in a tautomeric equilibrium with thiols, the thione forms of PyT predominate in solution at room temperature.[20–25] It is also interesting to compare the photochemical properties of PyT with thiones without N-atoms. Although there have been various recent reviews about the photoexcited thiones, we recognized a lack of systematic studies of the photochemistry and photophysics of N-containing thiones.[26,27]

In the present paper, we report the photochemical behavior, energy transfer, electron transfer, hydrogen abstraction and addition reaction, of PyT *via* ^{3}(PyT)* measured by nanosecond laser photolysis. Differences in reactivities between ^{3}(4PyT)* and ^{3}(2PyT)* to H-atom donors and alkenes are revealed. The electronic configuration of the lowest triplet states (T_1) were spectroscopically and kinetically characterized. Semi-empirical MO calculations on singlet and triplet excitations were carried out and compared with the experimental spectroscopic data.

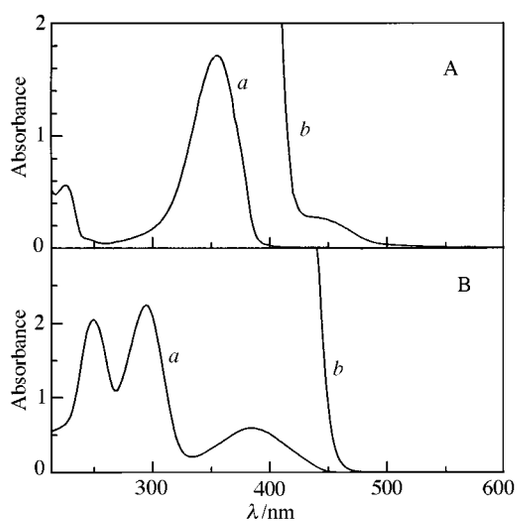

Fig. 1 Steady UV–VIS spectra of A, 4PyT and B, 2PyT in THF (1.0 cm optical path); *a*, 2.0×10^{-4} mol dm^{-3} and *b*, 5.0×10^{-3} mol dm^{-3}

Results and discussion

Steady-state absorption and phosphorescence spectra

The absorption spectra of 4PyT in THF are shown in Fig. 1A. The lowest-energy band at 420–500 nm is weak in intensity (ε = 60–70 dm^3 mol^{-1} cm^{-1}) and shows a blue shift on going from solution in THF to solution in ethanol. This band is characteristic of the >C=S chromophore of thiones and is assignable to the transition ^{1}(n–π*).[1,26,27] The next transition at 360 nm has an intense absorption (ε = 8700 dm^3 mol^{-1} cm^{-1}) assignable to the transition ^{1}(π–π*).[1,26,27]

2PyT in THF solution (Fig. 1B) shows intense absorption bands with maxima at 250 (ε = 10 300 dm^3 mol^{-1} cm^{-1}), 293

Table 1 Absorption maximum (λ_{max}), intrinsic triplet lifetime (τ_T^0), and self-quenching rate constants (k_{sq}) of ^{3}(4PyT)* and ^{3}(2PyT)* in various solvents

	^{3}(4PyT)*			^{3}(2PyT)*		
Solvent	λ_{max} [a]/nm	τ_T^0 [b]/μs	k_{sq} [b]/dm^3 mol^{-1} s^{-1}	λ_{max} [a]/nm	τ_T^0 [b]/μs	k_{sq} [b]/dm^3 mol^{-1} s^{-1}
Benzene	433 [c]	4.0	— [d]	464 [c]	2.50	4.7×10^9
THF	430	1.53	3.3×10^9	462	2.11	2.2×10^9
Pr^{i}OH	427	1.00	2.3×10^9	458	1.80	1.9×10^9
Acetonitrile	428	4.51	1.1×10^{10}	455	1.80	4.6×10^9

[a] Each λ_{max} value contains an estimation error of ±2 nm. [b] The intrinsic triplet lifetime (τ_T^0) was estimated by the extrapolation to infinite dilution in the plots of k_T ($1/\tau_T$) *vs.* [PyT]; k_{sq} was evaluated from the slope. Estimated errors of k_{sq} and τ_T are ±5%. [c] The ε values in benzene were estimated to be 6700 and 7140 dm^3 mol^{-1} cm^{-1} for ^{3}(4PyT)* and ^{3}(2PyT)*, respectively. [d] Because of low solubility of 4PyT in benzene, k_{sq} was not obtained.

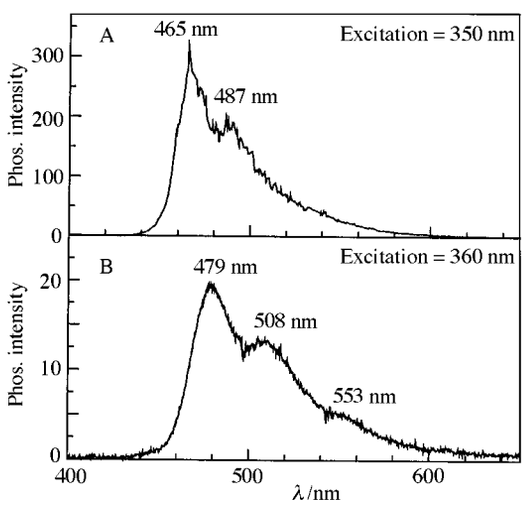

Fig. 2 Phosphorescence spectra observed at 77 K in glassy ethanol of A, 4PyT and B, 2PyT

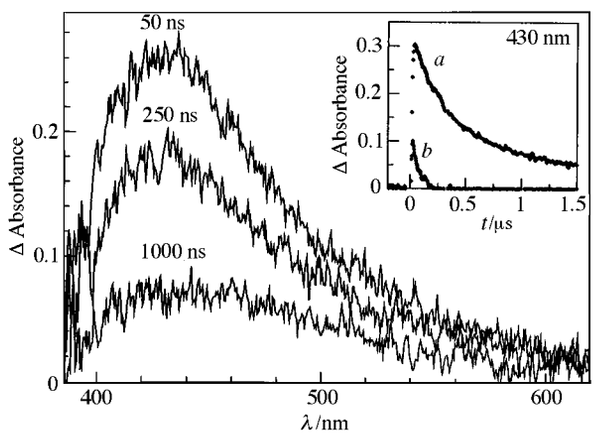

Fig. 3 Transient absorption spectra observed after laser photolysis of 4PyT (1.0×10^{-4} mol dm^{-3}) with 355 nm light in Ar-saturated acetonitrile. Insert: time-profiles of absorption band; *a*, in Ar-saturated and *b*, aerated solutions.

($\varepsilon = 11\,200$ dm^3 mol^{-1} cm^{-1}) and 385 nm ($\varepsilon = 2900$ dm^3 mol^{-1} cm^{-1}). These bands are assignable to the transition $^1(\pi$–$\pi^*)$.[1,26,27] The transition $^1(n,\pi^*)$ was not observed even at a higher concentration. The $^1(n$–$\pi^*)$ transition may be very weak and hidden by the intense band at 385 nm (Fig. 1B).

The spectral shape of a dilute 2PyT solution (5×10^{-5} mol dm^{-3}) is the same as that of a concentrated solution (up to 1.0×10^{-3} mol dm^{-3}). The absorption intensities, however, show a saturation with an increase in concentration to near 6×10^{-4} mol dm^{-3}. These findings suggest that aggregation may take place at a concentration range higher than (6–8) $\times 10^{-4}$ mol dm^{-3}, although the interaction between 2PyT molecules is not strong enough to alter the band shape. For 4PyT, a linear increase of the absorption intensity was observed up to a higher concentration (1.0×10^{-3} mol dm^{-3}) with the same spectral shape, suggesting that aggregation is not appreciable until 1.0×10^{-3} mol dm^{-3}.

We could not find fluorescence for either PyT at room temperature, which indicates that PyT have quite different electronic structures from other thiones which do not have an N-atom. The phosphorescence spectra of PyT in glassy ethanol at 77 K were recorded with excitation at 350–360 nm (Fig. 2). The relatively sharp phosphorescence bands were observed at 465 and 487 nm for ^{3}(4PyT)*. Rather broad phosphorescence bands were observed for ^{3}(2PyT)* at 479 nm (maximum) and 508 nm with a shoulder at 553 nm. The triplet energies (E_{T_1}) were estimated from the first phosphorescence peak to be 60.0 and 58.0 kcal mol^{-1} for ^{3}(4PyT)* and ^{3}(2PyT)*, respectively. When phosphorescence spectra were observed in 2-methyltetrahydrofuran (MeTHF) glass at 77 K, the peaks shifted to longer wavelength for ^{3}(4PyT)*, indicating that the lowest triplet state has $^3(n,\pi^*)$ character.[1,26] For ^{3}(2PyT)*, however, the phosphorescence peaks in MeTHF glass did not appreciably shift. Hence, the lowest triplet state of ^{3}(2PyT)* is $^3(\pi,\pi^*)$ in character.[1,26]

Laser flash photolysis

Transient absorption spectra observed by laser photolysis of 4PyT in Ar-saturated acetonitrile show a broad absorption with a broad peak around 430 nm with the absorption tail extending until 600 nm as shown in Fig. 3. The absorption intensity of the band decreases within a few μs. The shape of the transient absorption band changes at *ca.* 1 μs after the laser-shot, suggesting the formation of a secondary minor transient species. The transient absorption band at 430 nm was quenched very quickly in the presence of oxygen (Insert in Fig. 3) and other triplet quenchers, suggesting that the 430 nm absorption is due to the triplet–triplet (T–T) transition of ^{3}(4PyT)* [eqn. (1)]. The

$$\text{PyT} \xrightarrow{h\nu(355\text{ nm})} {}^1(\text{PyT})^* \xrightarrow{k_{isc}} {}^3(\text{PyT})^* \qquad (1)$$

λ_{max} values of the T–T absorption band observed in some solvents are summarized in Table 1. The intersystem crossing (ISC) process was not observed by nanosecond laser photolysis, indicating that k_{isc} is as large as *ca.* 10^8 s^{-1}.

In the presence of O_2, the decay rates of the transient absorption band at 430 nm increase (Insert in Fig. 3). From these decay rates the second-order rate constant was evaluated to be $k_{O_2} = 3.9 \times 10^9$ mol^{-1} dm^3 s^{-1} [eqn. (2)]. For quenching with O_2, it is reported that electron transfer takes place *via* ^{3}(PyT)* yielding $O_2^{\bullet -}$, which was identified by the spin-trapping method.[24] In our study, formation of singlet oxygen ($^1O_2$) was also confirmed by consumption of 1,3-diphenylisobenzofuran (DPBF).[28] Determination of the quantum yield of $^1O_2$-formation is described in a later section.

$$^3(\text{PyT})^* + O_2 \xrightarrow{k_{O_2}} \begin{cases} \rightarrow \text{PyT} + {}^1O_2 \\ \rightarrow \text{PyT}^{\bullet +} + O_2^{\bullet -} \end{cases} \qquad (2)$$

Table 2 Rate constants (k_q) for reactions of ^{3}(4PyT)* and ^{3}(2PyT)* with triplet quenchers and reactants at 23 °C in THF

Quencher	E_{T_1}/kcal dm^3 mol^{-1}	^{3}(4PyT)* k_q/ dm^3 mol^{-1} s^{-1}	^{3}(2PyT)* k_q/ dm^3 mol^{-1} s^{-1}	Reaction type
β-Carotene	19.4[b]	2.1×10^{10}	2.7×10^{10}	T-energy transfer
O_2	22.5[d]	3.1×10^{9}	3.9×10^{9}	T-energy transfer
Ferrocene	42.9[c]	4.4×10^{9}	5.9×10^{9}	T-energy transfer
1,3-CHD[a]	52.4[d]	5.9×10^{9}	5.1×10^{9}	T-energy transfer
Benzil	54.3[d]	6.2×10^{8}	3.8×10^{8}	T-energy transfer
Isoprene	60.1[d]	6.0×10^{7}	6.1×10^{7}	T-energy transfer
1,4-CHD[a]	78.0[e]	6.7×10^{8}	3.0×10^{7}	H-abstraction

Estimated errors of k_q are ±5%. [a] CHD: cyclohexadiene. [b] Ref. 29. [c] Ref. 30. [d] Ref. 31. [e] Ref. 32.

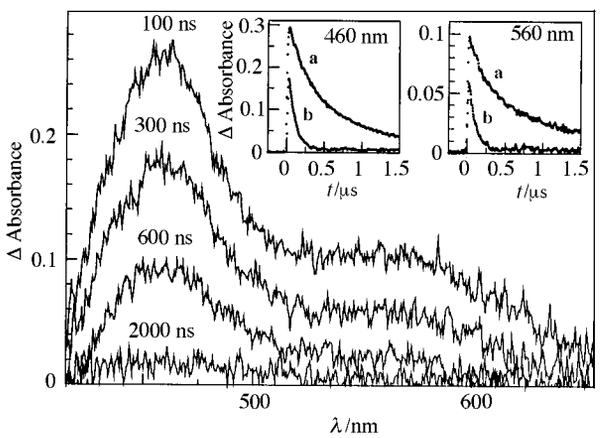

Fig. 4 Transient absorption spectra observed after laser photolysis of 2PyT (1.0×10^{-4} mol dm^{-3}) with 355 nm light in Ar-saturated acetonitrile. Insert: time-profiles of absorption bands; *a*, in Ar-saturated and *b*, aerated solutions.

The transient absorption spectra observed by laser photolysis of 2PyT in Ar-saturated acetonitrile are similar and show an absorption band around 460 nm with a weak band at 560 nm as shown in Fig. 4. The absorption intensities of both bands decrease within a few μs. From the quenching by O_2 (Insert in Fig. 4), the absorption bands at 460 and 560 nm are designated as due to the T–T transition of ^{3}(2PyT)* [eqn. (1)].

Self-quenching of ^{3}(PyT)*

Self-quenching [eqn. (3)] is one of the characteristics of the

$$^3(\text{PyT})^* + \text{PyT} \xrightarrow{k_{sq}} \text{PyT} + \text{PyT} \qquad (3)$$

triplet states of thiones.[4] The triplet decay lifetimes (τ_T) of ^{3}(PyT)* were measured as a function of ground-state PyT concentrations with low laser powers [$(2.0–5.0) \times 10^{-3}$ J pulse^{-1}].

For the decay of ^{3}(PyT)*, the first-order rate constant ($k_T = 1/\tau_T$) increases with the concentration of PyT, obeying eqn. (4).[3]

$$1/\tau_T = 1/\tau_T^0 + k_{sq}[\text{PyT}] \qquad (4)$$

The self-quenching rate constant (k_{sq}) and the intrinsic triplet lifetime (τ_T^0) were evaluated from the slopes and the intercepts of linear regressions, eqn. (4), and are listed in Table 1.

The k_{sq} values seem to depend on the viscosity of the solvent, suggesting that they are close to the diffusion controlled limit. These k_{sq} values are similar to those reported for the xanthione triplet state in a perfluoroalkane solvent.[5] The τ_T^0 values are quite short compared with those of aromatic carbonyl compounds.[6] Such a short lifetime is one of the characteristics of the thione triplet states, because of a heavy atom effect due to the S-atom.[3–6] The τ_T^0 value for ^{3}(4PyT)* in propan-2-ol (Pr^{i}OH) is shorter than those in other solvents, since the H-abstraction reaction is included in τ_T^0.

On addition of other triplet quenchers,[29–32] the second-order rate constants [k_q in eqn. (5)] were evaluated from the pseudo-

$$^3(\text{PyT})^* + \text{quencher} \xrightarrow{k_q} \text{PyT} + {}^3(\text{quencher})^* \qquad (5)$$

first order plots. The k_q values thus obtained are summarized in Table 2. Although the k_q values for cyclohexa-1,3-diene (1,3-CHD; $E_{T_1} = 52.4$ kcal mol^{-1})[31] are still close to the diffusion controlled limit, those for benzil ($E_{T_1} = 54.3$ kcal mol^{-1})[31] are about 1/10 of the diffusion limit. For 2-methylbuta-1,3-diene (isoprene; $E_{T_1} = 60.1$ kcal mol^{-1}),[31] the rate constants are even smaller than those of benzil by a factor of 1/10. Since the k_q values depend on the difference between the T_1-energies, they are all attributed to the triplet energy-transfer rate constants. Therefore, the E_{T_1} values of both ^{3}(4PyT)* and ^{3}(2PyT)* are calculated to be about 55 kcal mol^{-1} using the Sandros equation,[33] which is in good agreement with those estimated from phosphorescence peaks to within *ca.* 2–3 kcal mol^{-1}.

On steady-light photolysis in the presence of isoprene, no change of absorption intensity of either 4PyT or 2PyT was observed, which confirmed that the bimolecular experimental rate constants for isoprene relate to the energy transfer from ^{3}(PyT)* to isoprene. Although E_{T_1} of cyclohexa-1,4-diene (1,4-CHD; $E_{T_1} = ca.$ 78 kcal mol^{-1})[32] is higher than that of isoprene, the rate constant for ^{3}(4PyT)* with 1,4-CHD is larger than that of isoprene. This indicates that H-atom abstraction of ^{3}(4PyT)* from 1,4-CHD takes place; thus, the rate constant evaluated in Table 2 is attributed to H-atom abstraction (k_h), which is similar to that reported for the xanthione triplet.[5]

Triplet quantum yield (Φ_T) and extinction coefficient (ε_T)

The quantum yield of the triplet formation (Φ_T) was evaluated by energy transfer from ^{3}(PyT)* to β-carotene using 355 nm excitation using that of benzophenone (BP) as a standard ($\Phi_T = 1$).[3,34] A benzene solution of PyT (1.0×10^{-4} mol dm^{-3}), whose concentration was optically matched at 355 nm with BP (1.0×10^{-3} mol dm^{-3}) to compensate for the optical filtration effect, was mixed with a known concentration of β-carotene [$(2.0–7.5) \times 10^{-5}$ mol dm^{-3}]. Although β-carotene absorbs a substantial fraction (30–50%) of the laser photons at 355 nm, its direct excitation does not result in any significant triplet formation of β-carotene, because of the negligible triplet yield.[3] The rate constants (k_{et}) for energy transfer from ^{3}(4PyT)* and ^{3}(2PyT)* to β-carotene were evaluated to be 2.1×10^{10} and 2.7×10^{10} dm^3 mol^{-1} s^{-1}, respectively, from the rise curves of ^{3}(β-carotene)* at 540 nm (Fig. 5). Then, the Φ_T values in benzene are evaluated to be 0.75 and 0.86 for ^{3}(4PyT)* and ^{3}(2PyT)*, respectively. These Φ_T values are similar to those reported for thiobenzophenone derivatives when the shorter wavelength bands around 350 nm were excited.[3]

We attempted to measure the k_{isc} values of PyT by picosecond laser photolysis method, because of their absence of the fluorescence. The transient absorption bands of ^{3}(4PyT)* and ^{3}(2PyT)* were observed after 35 ps laser excitation at 355 nm. From the rise time-profiles of ^{3}(4PyT)* and ^{3}(2PyT)*, the k_{isc} values were evaluated to be 6.9×10^9 and $>1 \times 10^{10}$ s^{-1}, respectively. These large k_{isc} values are due to the high spin-orbit coupling ability of the S-atom.[3–6] We find a trend that the greater the k_{isc} values, the higher the Φ_T values.

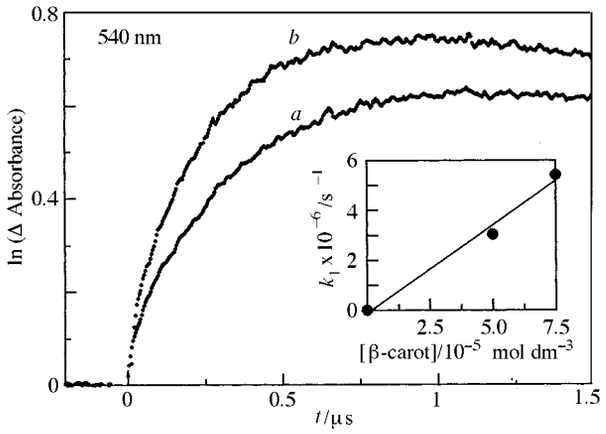

Fig. 5 Rise-time profiles at 540 nm of ^{3}(β-carotene)* obtained by laser photolysis of 2PyT (1.0×10^{-4} mol dm^{-3}) in Ar-saturated benzene in the presence of *a*, 5.0×10^{-5} and *b*, 7.5×10^{-5} mol dm^{-3} of [β-carotene]. Insert: pseudo-first order plot for triplet-energy transfer.

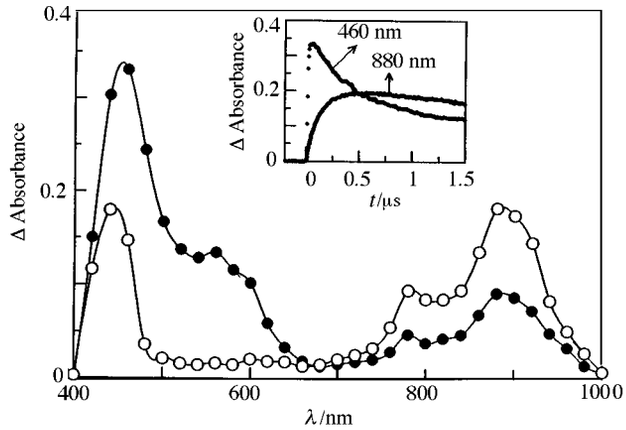

Fig. 6 Transient absorption spectra in the visible and near-IR region obtained by 355 nm laser photolysis of 2PyT (1.0×10^{-4} mol dm^{-3}) in the presence of 3,3′,5,5′-tetramethylbenzidine (1.0×10^{-3} mol dm^{-3}) in Ar-saturated acetonitrile; (●) 0.1 μs, (○) 1.0 μs. Insert: time-profiles of the absorption bands.

The molar extinction coefficient (ε_T) of ^{3}(PyT)* was estimated using the reported ε value (7220 mol^{-1} dm^3 cm^{-1})[34] of ^{3}(BP)* as a standard by substituting the observed Φ_T for PyT above. These ε values in benzene are determined to be 6700 mol^{-1} dm^3 cm^{-1} for ^{3}(4PyT)* at 430 nm and 7140 mol^{-1} dm^3 cm^{-1} for ^{3}(2PyT)* at 460 nm, respectively. These relatively large ε values are also characteristic of the triplet states of thiones.[3,5]

Quantum yield for $^1O_2$-formation

By using the Φ_T values estimated above, the quantum yield (Φ_o) for $^1O_2$-formation of ^{3}(PtT)* can be evaluated. Negative absorbance changes (ΔA_{DPBF}) due to the depletion of DPBF *via* its reaction with $^1O_2$ were observed at 440 nm when an O_2-saturated solution of PyT or BP, optically matched at 355 nm, was laser-photolysed in the presence of 5×10^{-5} mol dm^{-3} of DPBF. The absorbance changes were monitored at 440 nm by following the completion of the kinetics of depletion over *ca.* 10 μs. Under our experimental conditions, *ca.* 5% of the 355 nm laser photons were directly absorbed by DPBF and 95% of ^{3}(PyT)* decayed *via* interaction with $^1O_2$. Φ_o for PyT (Φ_o^{PyT}) was evaluated using eqn. (6). Based on the value of Φ_o^{BP} =

$$\Phi_o^{PyT} = \Phi_o^{BP} \frac{\Delta A_{DPBF}^{PyT} \Phi_T^{BP}}{\Delta A_{DPBF}^{BP} \Phi_T^{PyT}} \quad (6)$$

0.40,[3] we estimated $\Phi_o^{2PyT} = 0.61$ and $\Phi_o^{4PyT} = 0.65$. The high $^1O_2$-formation ability of ^{3}(PyT)* was confirmed by these results.

Triplet–triplet annihilation

When the laser power was increased under the same concentration of PyT, the initial decay rate increased and the decay-kinetics changed from first-order to second-order due to T–T annihilation. The slopes of the second-order plots yielded k_{TT}/ε, from which k_{TT} values are calculated to be 6.8×10^9 and 7.6×10^9 mol^{-1} dm^3 s^{-1} for ^{3}(4PyT)* and ^{3}(2PyT)* in benzene, respectively, by substituting the ε values estimated above. These k_{TT} values are close to the diffusion controlled limit in benzene ($k_d = 1.0 \times 10^{10}$ mol^{-1} dm^3 s^{-1}). At a higher concentration of PyT, T–T annihilation takes place concomitant with other reactions such as self-quenching.

Photoinduced electron transfer

The transient absorption spectra observed by laser photolysis of 2PyT in the presence of 3,3′,5,5′-tetramethylbenzidine (TMB) with 355 nm light in acetonitrile are shown in Fig. 6.

Sharp absorption peaks of ^{3}(2PyT)* at 460 and 560 nm are observed immediately after the laser flash decay along with the appearance of absorption bands at 780 and 880 nm which are assigned to TMB$^{\bullet+}$.[35,36a] The decay curve of ^{3}(2PyT)* at 460 nm and the rise curve of TMB$^{\bullet+}$ at 880 nm are shown in the insert in Fig. 6. The 460 nm band of ^{3}(2PyT)* did not decay completely due to its overlap with the rise absorption band of TMB$^{\bullet+}$ at 460 nm.[35,36a] From the rise curve of TMB$^{\bullet+}$ at 880 nm, the first-order rate constants were evaluated by curve-fitting with a single exponential. The second-order rate constant for electron transfer (k_{fet}) from TMB to ^{3}(2PyT)* [eqn. (7)]

$$^3(PyT)^* + TMB \xrightarrow{k_{fet}} PyT^{\bullet-} + TMB^{\bullet+} \quad (7)$$

can be evaluated by the [TMB]-dependence of the first-order rate constant as listed in Table 3.

For triphenylamine (TPA), no acceleration of the decay of ^{3}(2PyT)* was observed even in acetonitrile; the electron-transfer reaction does not occur. In the case of ^{3}(4PyT)*, on the other hand, the electron-transfer reaction takes place from both TMB and TPA in acetonitrile. The formation of 4PyT$^{\bullet-}$ was confirmed by the appearance of a band at 620 nm, because a similar absorption band was observed by γ-irradiation of 4PyT in MeTHF at 77 K.

In the presence of *p*-dinitrobenzenes (*p*-DNB) in Ar-saturated acetonitrile, the absorption band of ^{3}(PyT)* disappeared within a few hundred nanoseconds instead of the appearance of new absorption bands at 860 and 900 nm in the near-IR region. These rising absorption bands are attributed to the radical anion of *p*-DNB (*p*-DNB$^{\bullet-}$).[37,38] The rate constants (k_{obs}) thus obtained from the decay profiles of ^{3}(PyT)* by *p*-DNB are in good agreement with those obtained from the rise profiles of *p*-DNB$^{\bullet-}$ in acetonitrile. Thus, it is evident that the reaction rate constants for the quenching of ^{3}(PyT)* by *p*-DNB and for the formation of *p*-DNB$^{\bullet-}$ in acetonitrile can be attributed to the electron-transfer rate constants (k_{fet} in Table 3) from ^{3}(PyT)* to *p*-DNB [eqn. (8)].[36,37] Similarly, for *m*- and *o*-DNB, the k_{fet} values were evaluated.

$$^3(PyT)^* + p\text{-DNB} \xrightarrow{k_{fet}} PyT^{\bullet+} + p\text{-DNB}^{\bullet-} \quad (8)$$

When the time profiles were observed over long time-scales, the intensities of the absorption peaks of the radical ions (TMB$^{\bullet+}$ and *p*-DNB$^{\bullet-}$) decay slowly after reaching maxima in acetonitrile. These decays obeying second-order kinetics as shown in Fig. 7 can be attributed to the back electron-transfer reactions [eqns. (9) and (10)].[36,37]

$$PyT^{\bullet-} + TMB^{\bullet+} \xrightarrow{k_{bet}} PyT + TMB \quad (9)$$

Table 3 Rate constants for forward electron-transfer (k_{fet}) and back electron-transfer (k_{bet}) reactions in acetonitrile

Reactant	Donor	k_{fet}[a]/dm^3 mol^{-1} s^{-1}	(k_{bet}/ε)[b]/cm s^{-1}	k_{bet}/dm^3 mol^{-1} s^{-1}
4PyT	TMB	2.0×10^9	1.2×10^5	2.4×10^9
	TPA	1.9×10^9	4.5×10^5	3.2×10^9
	o-DNB	9.2×10^9	—[c]	—[c]
	m-DNB	8.2×10^9	—[c]	—[c]
	p-DNB	9.4×10^9	1.9×10^6	1.1×10^{10}
2PyT	TMB	1.7×10^9	1.1×10^5	2.2×10^9
	TPA	—[d]	—[d]	—[d]
	o-DNB	8.5×10^9	—[c]	—[c]
	m-DNB	7.6×10^9	—[c]	—[c]
	p-DNB	4.2×10^9	4.1×10^6	2.4×10^{10}

Estimated errors of k_{fet} and k_{bet} are ±5%. [a] Decays of ^{3}(4PyT)* and ^{3}(2PyT)* at 430 and 460 nm, respectively. [b] $\varepsilon_{TMB}{}^{\bullet+}$ = 20 200 dm^3 mol^{-1} cm^{-1} at 880 nm,[36a] $\varepsilon_{TPA}{}^{\bullet+}$ = 7100 dm^3 mol^{-1} cm^{-1} at 650 nm,[36b] and $\varepsilon_{DNB}{}^{\bullet-}$ = 5900 dm^3 mol^{-1} cm^{-1} at 900 nm[37] in acetonitrile. [c] The transient absorption bands of *o*-DNB$^{\bullet-}$ and *m*-DNB$^{\bullet-}$ overlapped with those of ^{3}(4PyT)* and ^{3}(2PyT)*. [d] Transient absorption band of ^{3}(2PyT)* disappeared in the presence of TPA.

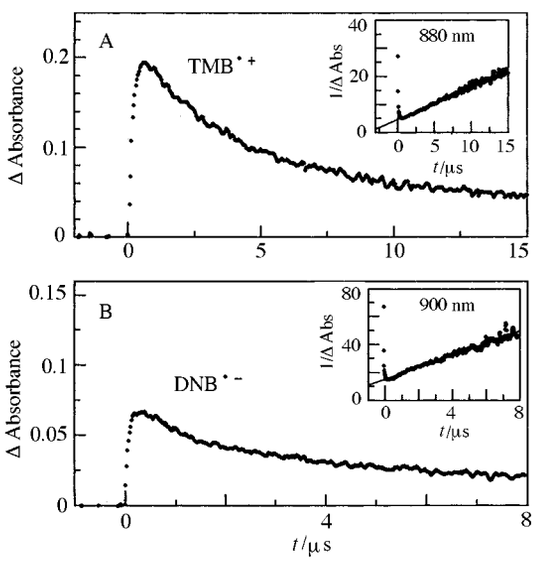

Fig. 7 Absorption–time profiles A, at 880 nm for the decay of TMB$^{\bullet+}$ and B, at 900 nm for the decay of *p*-DNB$^{\bullet-}$ obtained by 355 nm laser photolysis with 2PyT (1.0×10^{-4} mol dm^{-3}) in Ar-saturated acetonitrile. Insert: second-order plots.

$$PyT^{\bullet+} + p\text{-}DNB^{\bullet-} \xrightarrow{k_{bet}} PyT + p\text{-}DNB \qquad (10)$$

From the slopes of the second-order plots (Insert in Fig. 7), the ratio of the rate constant (k_{bet}) to molar extinction coefficient of radical ions (ε_r) can be obtained as listed in Table 3. On substituting the reported values of ε_r,[36,37] the k_{bet} values were evaluated for TMB$^{\bullet+}$ and DNB$^{\bullet-}$ in acetonitrile (Table 3).

H-Atom abstraction reaction of ^{3}(PyT)*

When 4PyT was solely photoexcited with 355 nm light in the presence of *p*-HO-C$_6$H$_4$-SH in Ar-saturated THF, the absorption intensity of ^{3}(4PyT)* decreases with the rise of the absorption band of *p*-HO-C$_6$H$_4$S$^{\bullet}$ at 520 nm[39–41] due to the H-atom abstraction of ^{3}(4PyT)* as shown in Fig. 8 [eqn. (11)]. With

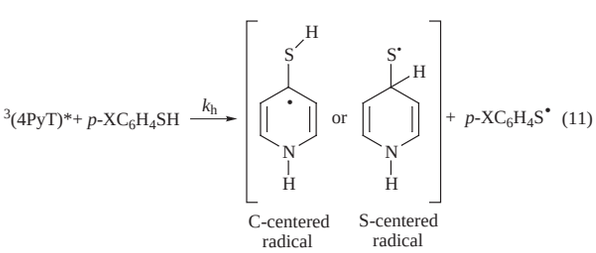

X = HH$_2$–, HO–, CH$_3$O-, *t*-C$_4$H$_9$–, H–, Cl–, Br–

Table 4 Rate parameters for hydrogen abstraction reactions (k_h) of ^{3}(PyT)* with different H-atom donors in THF and Hammett parameter σ^+ of *p*-X-C$_6$H$_4$-SH

H-Atom donor	λ_{max} of radical[a]/nm	(4PyT/k_h)/dm^3 mol^{-1} s^{-1}	(2PyT/k_h)/dm^3 mol^{-1} s^{-1}	σ^{+}[b]
p-NH$_2$-C$_6$H$_4$SH	580[d]	6.2×10^8	8.3×10^7	−1.3
p-HO-C$_6$H$_4$SH	520[d]	5.0×10^8	1.3×10^7	−0.92
p-CH$_3$O-C$_6$H$_4$SH	520[d]	4.8×10^8	8.9×10^6	−0.78
p-Bu^t-C$_6$H$_4$SH	490[d]	4.6×10^8	7.3×10^6	−0.26
C$_6$H$_5$SH	480[d]	4.0×10^8	7.9×10^5	0.0
p-Cl-C$_6$H$_4$SH	510[d]	3.8×10^8	3.4×10^5	0.11
p-Br-C$_6$H$_4$SH	510[d]	3.3×10^8	2.8×10^5	0.15
α-Tocopherol	420[e]	1.0×10^8	6.2×10^6	—[c]

Estimated errors of λ_{max} are ±2 nm and those of k_h are ±5%. [a] Substituted benzene thio radicals formed by H-atom abstraction of ^{3}(PyT)* from different H-atom donors. [b] σ^+ values are cited from ref. 40. [c] σ^+ value is neglected. [d] S-centered radicals were observed (refs. 39 and 40). [e] An O-centered radical was observed (ref. 42).

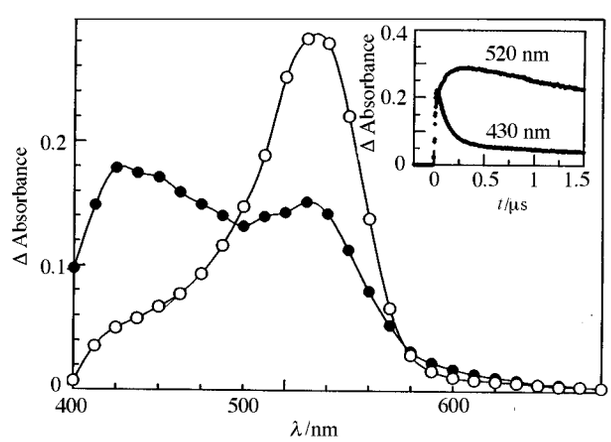

Fig. 8 Transient absorption spectra observed by laser photolysis (355 nm light by Si-PIN photodiode) of 4PyT (1.0×10^{-4} mol dm^{-3}) with *p*-HOC$_6$H$_4$SH (1.0×10^{-3} mol dm^{-3}) in Ar-saturated THF; (●) 50 ns, (○) 500 ns. Insert: decay profile of ^{3}(4PyT)* at 430 nm and rise profile of *p*-HOC$_6$H$_4$S$^{\bullet}$ at 520 nm.

other H-atom donors such as *p*-X-C$_6$H$_4$-SH or α-tocopherol, the formation of *p*-X-C$_6$H$_4$S$^{\bullet}$[39–41] or tocopheroxy radical[42] was observed by using the nanosecond laser photolysis method with a photomultiplier system.[19] The H-atom abstraction rate constants (k_h) of ^{3}(4PyT)* are summarized in Table 4 with the absorption maxima of the radicals formed from the different H-atom donors.

In the case of ^{3}(2PyT)*, slow H-atom abstraction reactions were observed from H-atom donors. The k_h values for ^{3}(2PyT)* (in Table 4) are smaller than those for ^{3}(4PyT)* by a factor 1/10–1/1000. There may be at least two factors controlling the

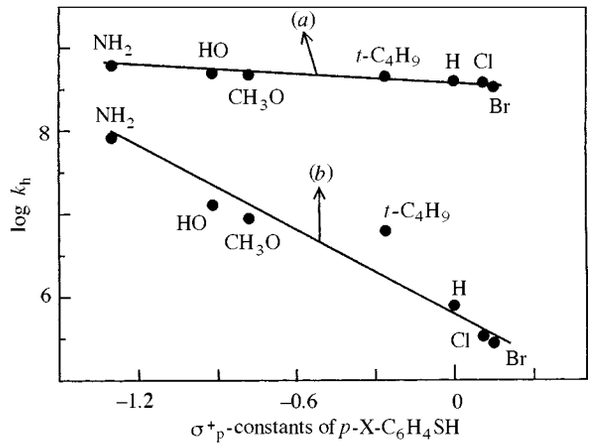

Fig. 9 Hammett plots of log k_h against σ^+-constants of p-XC_6H_4SH for reaction with (*a*) ^{3}(4PyT)* and (*b*) ^{3}(2PyT)* in Ar-saturated THF

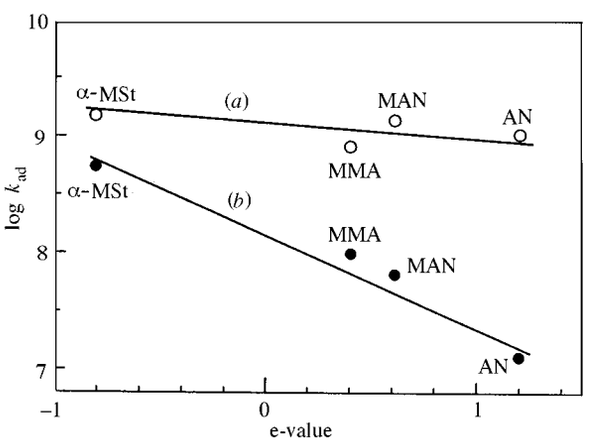

Fig. 10 Plots of log k_{ad} for ^{3}(PyT)* against Alfrey–Price's *e*-values of different alkenes in Ar-saturated THF; (*a*) for ^{3}(4PyT)* and (*b*) for ^{3}(2PyT)*

reactivities. One factor is steric hindrance caused by the close proximity of the H-atom of the H-donor with the S atom in ^{3}(2PyT)*, because of the intramolecular interaction between the H atom and the N atom in ^{3}(2PyT)*. The other is an electronic factor, for example, ^{3}(4PyT)* has reactive (n,π*) character, while ^{3}(2PyT)* has less reactive (π,π*) character. Both factors may be operating.

To investigate the substituent effect in the reactions of ^{3}(PyT)* with p-XC_6H_4-SH as the H-atom donor, Hammett plots of log k_h against σ^+-constants of p-X-C_6H_4SH were plotted and are shown in Fig. 9. Negative slopes [$\rho^+ = ca.\ -0.2$ for ^{3}(4PyT)* and $ca.\ -1.0$ for ^{3}(2PyT)*] for the Hammett relation [eqn. (12)][40] were observed, implying that the electrophilicity of ^{3}(2PyT)* is higher than that of ^{3}(4PyT)* with respect to H–S.

$$\Delta(\log k_h) = \rho^+\sigma^+_x \qquad (12)$$

The electrophilic nature of ^{3}(4PyT)* suggests that the S-atom is the active site for the H-atom abstraction reaction, since the aromatic and aliphatic thiyl radicals also have electrophilic nature.[40,43] Thus, this observation suggested that the C-centered radical [eqn. (11)] was formed by H-atom abstraction of ^{3}(4PyT)*.

Addition reaction to alkenes

The decay rates of ^{3}(PyT)* increase with increasing concentration of alkenes due to the reaction of ^{3}(PyT)*; cycloaddition is most probable as with other aromatic thiones.[8,43] The rate constants of the addition reaction (k_{ad}) with several alkenes are summarized in Table 5 with Alfrey–Price's *e*-values,[40] which are a measure of the electron density of C=C. Conjugated alkenes are more reactive than non-conjugated alkenes with ^{3}(PyT)*. The k_{ad} values for the addition reaction of ^{3}(PyT)* to various alkenes are plotted against Alfrey–Price's *e*-values as shown in Fig. 10.

Table 5 Addition reaction rate constants (k_{ad}) and Alfrey–Price's *e*-values of alkenes for the reaction with ^{3}(PyT)* in THF

Alkenes	(4PyT/k_{ad})[a]/ dm^3 mol^{-1} s^{-1}	(2PyT/k_{ad})[a]/ dm^3 mol^{-1} s^{-1}	*e*-Value[b]
CH_2=C(CH_3)Ph (α-MSt)	1.5×10^9	5.5×10^8	−0.81
CH_2=C(CH_3)CO_2CH_3 (MMA)	8.2×10^8	9.9×10^7	+0.40
CH_2=C(CH_3)CN (MAN)	1.4×10^9	6.6×10^7	+0.61
CH_2=CHCN (AN)	1.1×10^9	1.3×10^7	+1.20
CH_2=CHOBu (BVE)	5.0×10^8	3.2×10^7	−1.77
CH_2=CHOEt (EVE)	4.1×10^8	1.2×10^7	−1.17
CH_2=CHOCOCH$_3$ (VAc)	1.7×10^8	6.8×10^5	−0.22

[a] Estimated errors of k_{ad} are ±5%. [b] The *e*-values of alkenes are cited from ref. 40.

The slope of the plot is a measure of the polar character of the attacking ^{3}(PyT)*. Negative slopes suggest the electrophilicity of ^{3}(PyT)* with respect to C=C.[40–43] The electrophilic nature of ^{3}(PyT)* indicates that a partial charge transfer character is generated in the transition state during the addition of ^{3}(PyT)* to alkenes similar to the triplet state of xanthione.[43] Turro and Ramamurthy and others reported that thiones undergo cycloaddition with alkenes probably *via* step-wise processes [for example, eqn. (13) shows the reaction of ^{3}(4PyT)*].[2,8,43] The

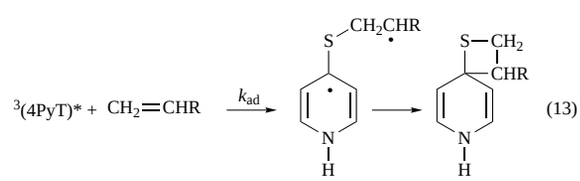

(13)

magnitude of the negative slope for ^{3}(2PyT)* is greater than that of ^{3}(4PyT)*, while the addition reactivity of ^{3}(4PyT)* to alkenes is higher than that of ^{3}(2PyT)*. These findings are similar to those for H-atom abstraction reactions. Thus, the initial bond formation with alkenes would be expected to be directed by the radical-like character of S-atom in ^{3}(PyT)*.

Steady-light photolysis

In order to clarify the different reactivities of ^{3}(4PyT)* and ^{3}(2PyT)*, the photochemical changes of PyT caused by steady-light (>310 nm) illumination were studied. By the steady photolysis of 4PyT in H-atom donor solvents or with H-atom donors, the thione band at 345 nm decreases slowly with irradiation time ($t_{\frac{1}{2}} = 41$ s in Ar-saturated propan-2-ol) accompanied by the appearance of a new band at 260 nm (Fig. 11) which is assigned to pyridine as confirmed by GC–MS and a characteristic UV-spectrum.[44] Bond cleavage between C–S of 4PyT was also confirmed by the formation of H_2S, which was chemically confirmed by the color change of $CuSO_4$ into a black precipitate of CuS. It was confirmed that H-atom donor solvents (*i.e.* Pr^{i}OH and THF) or additives (*i.e.* 1,4-CHD) are indispensable for the desulfurization reaction of 4PyT, since appreciable UV spectral change was not observed in poor H-atom donor solvents such as acetonitrile after photo-illumination for 2 h. On addition of triplet quenchers such as 1,3-CHD and benzil, the desulfurization reaction did not take place, suggesting that reaction takes place *via* ^{3}(4PyT)* followed by H-atom abstraction. An increase in the concentration of 4PyT slowed down the reactions suggesting that the practical lifetime of ^{3}(4PyT)* becomes short by self-quenching. A probable mechanism of the desulfurization reaction of 4PyT *via* ^{3}(4PyT)* is shown in

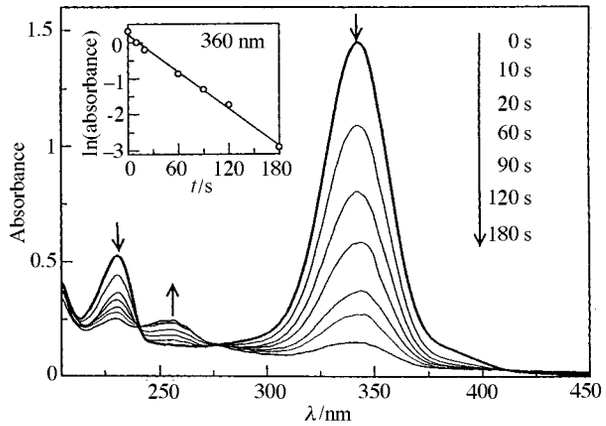

Fig. 11 Absorption spectral changes observed by steady photolysis of 4PyT (1.0×10^{-4} mol dm^{-3}) in Ar-saturated propan-2-ol with light longer than 310 nm. The absorption band at 260 nm is due to pyridine. Insert: first-order plot.

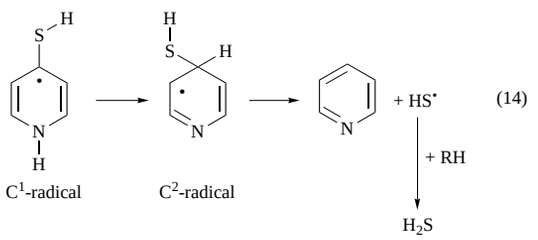

(14)

eqn. (14). A C^2-radical may be formed by a H-atom shift from a C^1-radical, in which the C–H bond may easily dissociate yielding stable pyridine and reactive HS$^\bullet$ which finally changes to H_2S.[19c]

In the case of 2PyT, UV-spectral change was not observed by steady-light (>310 nm) illumination (within 3–5 min) in H-atom donor solvents or with H-atom donors, suggesting that H-atom abstraction ability is very low as observed by laser photolysis.

MO calculations

The electronic transition energies of the singlet state of PyT were calculated by the restricted Hartree–Fock method on the geometries optimized at the MNDO/CI level using the MOPAC program package.[45] The first transition was predicted to be (n–π*) in character for 4PyT. This band was predicted to be located at 580 nm for 4PyT with low oscillation strength, which corresponds to the observed lowest energy transition at *ca.* 445 nm ($\varepsilon = 60$–70 dm^3 mol^{-1} cm^{-1}). For 2PyT, a similar (n–π*) transition was predicted at 530 nm, although such a transition was not observed as shown in Fig. 1B. The second transitions were predicted to be (π,π*) in character at 345 nm for 4PyT and at 380 nm for 2PyT with very high oscillation strength, corresponding to the observed absorptions at 360 and 383 nm, respectively.

The electron density of ^{3}(PyT)* was calculated by the unrestricted open-shell Hartree–Fock (ROHF) method on the geometries optimized at the MNDO level.[45] For both ^{3}(4PyT)* and ^{3}(4PyT)*, there are two singly occupied levels (SOMO). In the case of ^{3}(2PyT)*, the electron density of C=S at the lower SOMO level is located at p_x (or p_y) plane (n-character), while the upper SOMO level is p_z-plane (π-character). This indicates the ^{3}(n,π*)-configuration of the lowest level for ^{3}(4PyT)*, which is in good agreement with the observed blue shift (changing solvent polarity) of phosphorescence bands. For ^{3}(2PyT)*, the electron density of S-atom is distributed on the p_z-plane (π-character) in both the lower and upper SOMO levels, indicating that the electronic configuration is ^{3}(π,π*) in character. This also corresponds with the ^{3}(π,π*) electronic configuration evaluated by the negligibly small shift of phosphorescence.

Conclusion

Most of the properties of the excited triplet states of ^{3}(PyT)* are common with those of thiones without an N-atom, although the non-fluorescent excited singlet states are different. Compared with pyridinones, the Φ_T values of ^{3}(PyT)* are high, suggesting the importance of the triplet states in photochemistry of pyridinethione. The relatively high values of the lowest triplet state energy (E_{T_1}) are one of the origins of high electron transfer abilities. The photochemical reactivities of ^{3}(4PyT)* to H-atom donors or to alkenes are quite higher than those of ^{3}(2PyT)*, which may be related to the steric effect and/or to electronic configuration; *i.e.* ^{3}(4PyT)* having the ^{3}(n,π*)-configuration is more reactive than ^{3}(2PyT)* with the ^{3}(π,π*)-configuration. The electrophilicity shows the opposite tendency. The substituent effects also revealed that the S-atom is the reactive center of ^{3}(PyT)* for both H-atom abstraction and addition reactions.

Experimental

Materials and steady-state measurements

Solvents used for the transient absorption measurements were of spectroscopic grade. Pyridine-2(1*H*)-thione (2PyT) and pyridine-4(1*H*)-thione (4PyT) were obtained from Aldrich Chemical Co. in a purity of 99%. 3,3′,5,5′-Tetramethylbenzidine (TMB), triphenylamine (TPA) and dinitrobenzenes (DNB) were purified by recrystallization. Commercially available various triplet quenchers, H-atom donors and alkenes (purity >98%) were used.

Absorption spectra were followed using a UV–VIS spectrophotometer with an appropriate optical path. Phosphorescence spectra were measured in frozen glassy media at 77 K. The photolysed solution of 4PyT in the presence of H-atom donors was analyzed using a GC–MS spectrometer; an observed intense GS peak was assigned to pyridine with $M = 79$.

Transient absorption measurements

The nanosecond time-scale laser photolysis apparatus was of a standard design with THG (355 nm) light of Nd:YAG laser (Quanta-Ray, GCR-130, 6 ns FWHM).[19] Transient spectra were recorded with a multichannel photodiode (MCPD) system and time profiles were followed by a photomultiplier system (PMT) in the visible region. In the near-IR region, a Ge-APD (germanium avalanche photodiode, Hamamatsu, B2834) module detector attached to a monochromator was employed, using a pulsed Xe-lamp (15 J pulse^{-1}, 60 μs FWHM) as a probe light. Picosecond laser photolysis was performed with a mode-lock Nd:YAG laser (35 ps duration). The transient absorption spectra was observed by monitoring light from Xe break-down with a streak camera detector.[37] Deaerated solutions were obtained by Ar-bubbling in a rectangular quartz cell with a 10 mm optical path. All measurements were carried out at 23 °C.

Acknowledgements

The present work was partly supported by the Grant-in-Aid on Priority-Area-Research on 'Carbon Alloys' (No. 09243201) from the Ministry of Education, Science, Sports and Culture. The authors would like to thank Takeda Science Foundation.

References

1 J. Wirz, *J. Chem. Soc., Perkin Trans. 2*, 1973, 1307.
2 P. de Mayo, *Acc. Chem. Res.*, 1976, **9**, 52.
3 C. V. Kumar, L. Qin and P. K. Das, *J. Chem. Soc., Faraday Trans. 2*, 1984, **80**, 783.
4 A. Maciejewski, D. R. Demmer, D. R. James, A. Safarzadeh-Amiri, R. E. Verrall and R. P. Steer, *J. Am. Chem. Soc.*, 1985, **107**, 2831.
5 K. Bhattachayya, V. Ramamurthy and P. K. Das, *J. Phys. Chem.*, 1987, **91**, 5626.

6 A. Maciejewski, M. Syzmanski and R. P. Steer, *J. Phys. Chem.*, 1988, **92**, 6939.
7 R. Minto, A. Samanta and P. K. Das, *Can. J. Chem.*, 1989, **67**, 967.
8 J. Kamphuis, H. J. T. Bos, R. J. Visser, B. H. Huizer and C. A. G. O. Varma, *J. Chem. Soc., Perkin Trans. 2*, 1986, 1867.
9 D. H. R. Barton, D. Crich and W. B. Motherwell, *Tetrahedron*, 1985, **41**, 3901.
10 D. H. R. Barton and S. Z. Zard, *Pure Appl. Chem.*, 1986, **58**, 675.
11 M. Newcomb and U. Park, *J. Am. Chem. Soc.*, 1986, **108**, 4132.
12 M. Newcomb and J. Kaplan, *Tetrahedron Lett.*, 1987, **28**, 1615.
13 J. Boivin, E. Crepon and S. Z. Zard, *Tetrahedron Lett.*, 1990, **31**, 6869.
14 E. Shaw, J. Bernstein, K. Loser and W. A. Lott, *J. Am. Chem. Soc.*, 1950, **72**, 4362.
15 A. Albert, *Selective Toxicity: The Physico-Chemical Basis of Therapy*, Chapman and Hall, London, 7th edn., 1985.
16 G. J. Kontoghiorghes, A. Piga and A. V. Hoffbrand, *Hematol. Oncol.*, 1986, **4**, 195.
17 W. Adam, J. Cadet, F. Dall'Acqua, D. Ramaiah and C. R. Saha-Moller, *Angew. Chem.*, 1995, **107**, 91.
18 K. J. Reszka and C. F. Chignell, *Photochem. Photobiol*, 1994, **60**, 442.
19 (*a*) A. Watanabe and O. Ito, *J. Phys. Chem.*, 1994, **98**, 7736; (*b*) M. M. Alam, A. Watanabe and O. Ito, *J. Org. Chem.*, 1995, **60**, 3440; (*c*) M. M. Alam, M. Fujitsuka, A. Watanabe and O. Ito, *J. Phys. Chem.*, 1998, **102**, 1338.
20 R. A. Jones and A. R. Katritzky, *J. Chem. Soc.*, 1960, 2937.
21 P. Beak, J. B. Covington and S. G. Smith, *J. Am. Chem. Soc.*, 1976, **98**, 8284.
22 P. Beak, J. B. Covington and J. M. White, *J. Org. Chem.*, 1980, **54**, 1347.
23 P. Beak, J. B. Covington, S. G. Smith, J. M. White and J. M. Zeigler, *J. Org. Chem.*, 1980, **54**, 1354.
24 S. Stoyanov, I. Petkov, L. Antonov and T. Stoyanov, *Can. J. Chem.*, 1990, **68**, 1482.
25 M. J. Nowak, L. Lapinski, H. Rostowska, A. Les and L. Adamowicz, *J. Phys. Chem.*, 1990, **94**, 7406.
26 V. Ramamurthy and R. P. Steer, *Acc. Chem. Rev.*, 1988, **21**, 380.
27 A. Maciewjewski and R. P. Steer, *Chem. Rev.*, 1993, **93**, 67.
28 H. H. Wasserman and R. W. Murray, in *Singlet Oxygen*, Academic Press, New York, 1979, ch. 5, 6, 8 and 9.
29 C. Lambert and R. W. Redmond, *Chem. Phys. Lett.*, 1994, **228**, 495.
30 A. Farmilo and F. Wilkinson, *Chem. Phys. Lett.*, 1975, **34**, 575.
31 S. I. Murov, *Handbook of Photochemistry*, Marcel Dekker, New York, 1973.
32 Evaluated from T_1 of but-2-ene.[31]
33 K. Sandros, *Acta Chem. Scand.*, 1964, **18**, 2355.
34 A. A. Lamola and G. S. Hammond, *J. Chem. Phys.*, 1965, **43**, 2129.
35 A. Watanabe, O. Ito and K. Mori, *Synth. Met.*, 1989, **32**, 237.
36 (*a*) Y. Sasaki, Y. Yoshikawa, A. Watanabe and O. Ito, *J. Chem. Soc. Faraday Trans.*, 1995, **91**, 2287; (*b*) $\varepsilon_{TPA}{}^{\bullet+}$ was determined by comparing the transient absorption band of $TPA^{\bullet+}$ at 650 nm with the transient band of $^3C_{60}$* at 740 nm ($\varepsilon_{^3C_{60}^*} = 16\,000$ dm^3 mol^{-1} cm^{-1}; M. M. Alam, A. Watanabe and O. Ito, *J. Photochem. Photobiol. A*, 1997, **104**, 59).
37 M. Fujitsuka, T. Sato, T. Shimidzu, A. Watanabe and O. Ito, *J. Phys. Chem. A*, 1997, **101**, 1056.
38 T. Shida, *Electronic Absorption Spectra of Radical Ions*, Physical Science data 34, Elsevier, Amsterdam, 1988.
39 (*a*) O. Ito and M. Matsuda, *J. Am. Chem. Soc.*, 1979, **101**, 1815; (*b*) O. Ito and M. Matsuda, *J. Am. Chem. Soc.*, 1979, **101**, 5732; (*c*) O. Ito and M. Matsuda, *J. Am. Chem. Soc.*, 1982, **104**, 1815.
40 (*a*) O. Ito, *Res. Chem. Intermed.*, 1995, **21(1)**, 69; (*b*) H. Yoshizawa, O. Ito and M. Matsuda, *Br. Polym. J.*, 1988, **20**, 441.
41 (*a*) M. M. Alam, H. Konami, A. Watanabe and O. Ito, *J. Chem. Soc., Perkin Trans. 2*, 1996, 263; (*b*) G. R. Dey, D. B. Naik, K. Kishore and P. N. Moorthy, *Res. Chem. Intermed.*, 1995, **21(1)**, 47.
42 F. Bohm, R. Edge, E. J. Land, D. J. McGarvey and T. G. Truscott, *J. Am. Chem. Soc.*, 1997, **119**, 621.
43 N. J. Turro and V. Ramamurthy, *Tetrahedron Lett.*, 1976, **28**, 2423.
44 *UV Atlas of Organic Compounds*, Verlag Chemie, Butterworths, 1968, vol. II, G5/1,2.
45 (*a*) J. J. P. Stewart, *J. Comput. Chem.*, 1989, **10**, 209; (*b*) J. J. P. Stewart, *Quantum Chemistry Program Exchange Bull.*, 1989, **9**, 10.

Paper 7/08472B
Received 24*th November* 1997
Accepted 27*th January* 1998